Cror blade deformation, part 2: Aeroelastic computations and comparison with experiments

Y. Mauffrey, A. Geeraert, S. Verley

IFASD 2015
International Forum on Aeroelasticity and Structural Dynamics
June 28 — July 02, 2015 ▲ Saint Petersburg, Russia

CROR BLADE DEFORMATION, PART 2: AEROELASTIC COMPUTATIONS AND COMPARISON WITH EXPERIMENTS

Y. Mauffrey[1], A. Geeraert[1], S. Verley[1]

[1] ONERA
The French Aerospace Lab, 92322 Châtillon, France

yann.mauffrey@onera.fr

Keywords: experimental, validation, aeroelasticity, structural dynamics.

Abstract: The present paper is dedicated to the numerical prediction of contra-rotating open rotors, CROR, blade deformations and the correlations with experimental data, in cruise conditions. The major challenge of this study lies in the nonlinear nature of the CROR blades aeroelastic behavior. Aerodynamic and centrifugal loadings on CROR blades may result in large deflection at blade tip and geometric nonlinearities have to be taken into account. In this paper we investigate the impact of these kinds of nonlinearities in static deformation numerical predictions.

1 INTRODUCTION

Although contra-rotating open rotors (CROR) came into service mainly in the 40's, even widely in some countries, and with enhanced performances compared to single propellers, their complex design, installation and maintenance prevented them from being used over an extended period of time. The current research by aeronautical community on bringing significant step changes regarding the environmental impact of aviation has given new impetus to this kind of propulsion system. Within the CleanSky SFWA-ITD project, recent wind tunnel tests campaigns have been performed to get a deeper understanding of the complex phenomena involving aerodynamic, acoustic, structural, performances, and aeroelastic topics. A part of this project was then dedicated to correlation between numerical simulation and experimental results.

ONERA aeroelasticity department was involved in experimental measurement of blade deflection [1] and part of a working group, also composed of DLR [7] and NLR, named to perform aeroelastic analysis using high fidelity Computational Fluid dynamics (CFD) and computational Structural Mechanics (CSM) Tools.

The present study focuses on the numerical prediction of CROR blade displacements at cruise conditions. This paper presents static aeroelastic computational results obtained at ONERA with the elsA solver and their correlation with experimental data.

2 NUMERICAL MODEL

Aeroelasticity is the study of the interactions between elastic, inertial and aerodynamic forces. elsA's aeroelastic module [8] is able to solve several kinds of aeroelastic simulations: prediction of coupled equilibrium of steady aerodynamic forces and static deformations of structures possibly under gravity effects and prediction of the dynamic aeroelastic stability using a weak or a strong coupling approach. Before 2015, two methodologies were implemented in the elsA aeroelastic module to solve the structure: a modal decomposition

approach, or a flexibility matrix approach. Both of these methods suppose that the structure has a linear behaviour. Recent developments in the code provide the capability of plugging an external FEM solver to the elsA aeroelastic module via a python interface for steady and unsteady computations. With such a development aeroelastic computations can be performed considering both CFD and CSM parts as nonlinear.

2.1 Flow solver and mesh grid

The CROR CFD geometry is a single channel reduction for both Front and Rear rotor. To avoid the unsteadiness due to the blade passage, mixing plane boundary condition is imposed between the front row and the rear row. With this assumption the CFD computations should converge to a steady solution.

The CFD computations are performed with the elsA code which is based on a cell centered approach on structured multiblock meshes. More information about this flow solver can be found in [3]. For steady RANS simulations convective fluxes are computed with a second order centered scheme with classical artificial dissipation parameter k^2 and k^4 [4]. Diffusive fluxes are computed with a second order centered scheme. The pseudo time marching is performed by using an implicit backward Euler scheme and a scalar Lower-Upper (LU) Symmetric Successive Over-relaxation (SSOR) as proposed in [6]. The turbulent viscosity is computed with the k-omega model of Kok [5].

The flow domain is discretized using a multiblock approach. Putting aside the mixing plane boundaries, all blocks of the configuration have conformal interfaces. An overview of the computational domain is presented in figure 1, the green zone is the front row domain and the orange zone is the rear row domain. The blades are depicted in blue and a zoom on the front rotor and rear rotor interfaces are presented in figure 2. On this picture the block edges are depicted in black. The structured grid contains about 4 million nodes, and is split into 57 blocks, 28 blocks for the front blade and 27 blocks for the rear blade. The CFD problem is solved in parallel on 28 processors.

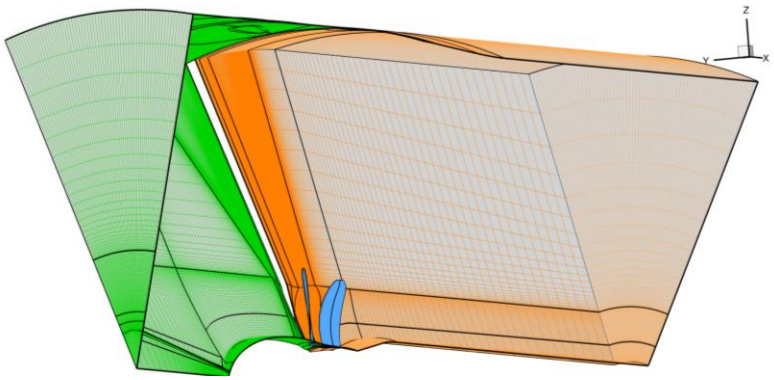

Figure 1: Overview of the computational domain

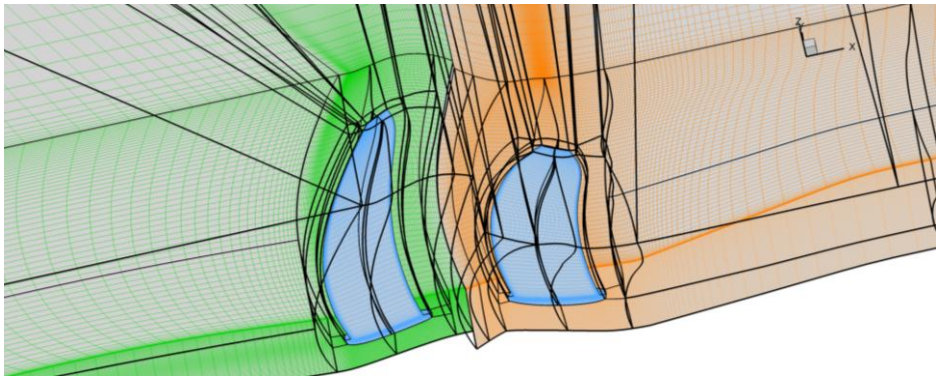

Figure 2: Zoom on the front rotor and rear rotor interface

2.2 Finite Element Model (FEM) tuning

2.2.1 Background & objectives

Once the Z49 CROR wind tunnel tests (WTT) with Airbus AI-PX7 generic blades [2] ended, it has been decided to correlate aeroelastic computational methods with experimental results obtained by SPA [1]. In particular, improving the representativeness of blade structural model (FEM) has been jointly supported by NLR and ONERA.

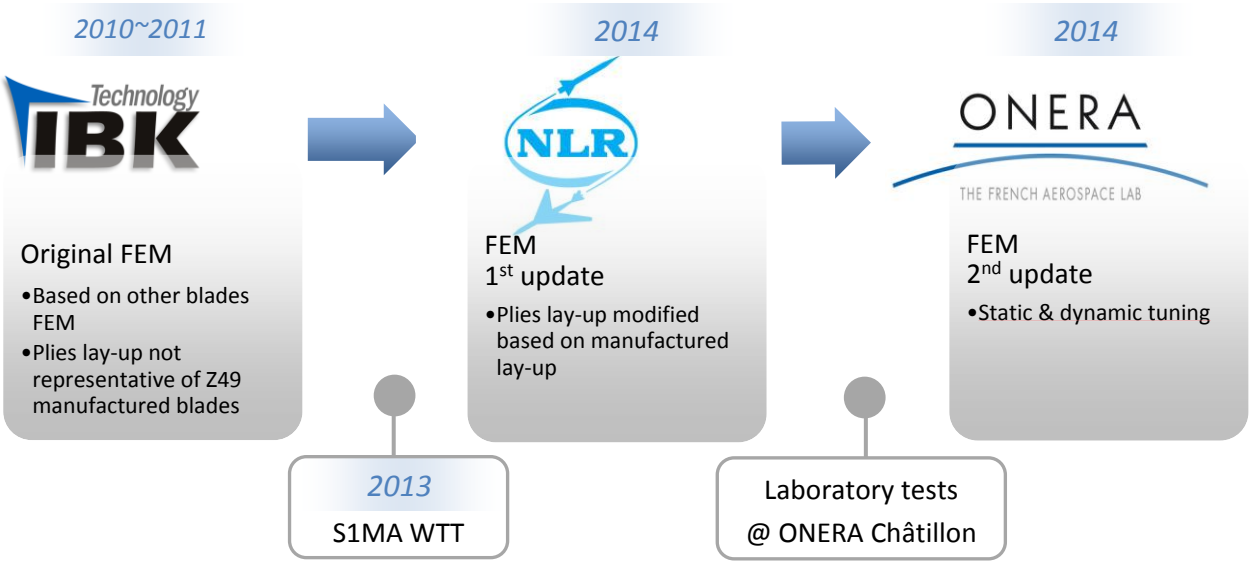

Figure 3 - Evolution of Z49 blades FEM

2.2.2 Static and dynamic tuning

FEMs were initially built by IBK, homothetically from other blade FEMs, more by easiness and quickness at that time than by representativeness considerations. The first improvement by NLR (manufacturer of the blades) has consisted in correcting the plies lay-ups of the front and rear blades such as they are representative of the manufactured lay-ups (number of plies, shapes, thickness, orientations, additional plies). The second improvement by ONERA has been the static and dynamic tuning, using the optimization solution MSC NASTRAN SOL200, and taking the dedicated laboratory tests (static and dynamic) results as reference. A sensitivity study has been performed to determine the minimal set of optimization variables,

for computational efficiency and performance. Constraints on static deflection and modal frequencies and shapes have also been added to guide the problem-solving to acceptable solutions with desired level of accuracy. Static and dynamic correlations between experimental results and numerical results from the optimized FEM are shown for the rear blade in figure 4, figure 5 and table 1, exhibiting less than 7% of difference on static deflections (among 2 loadcases) and a correlation up to seven modes with less than 6% of relative difference for frequencies and a MAC number greater than 0.9 for almost all concerned modes. Correlations for the front blade are better for both ONERA and NLR FEMs.

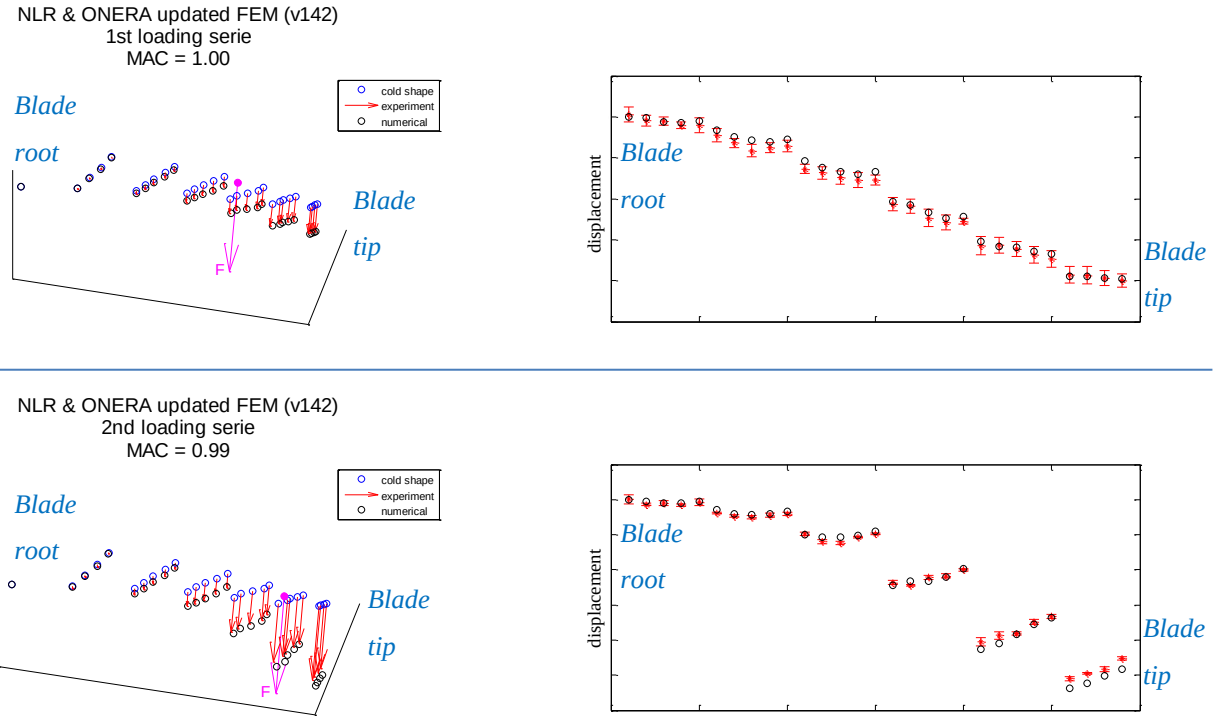

Figure 4 - Status after ONERA FEM fine-tuning – Rear blade – Static results

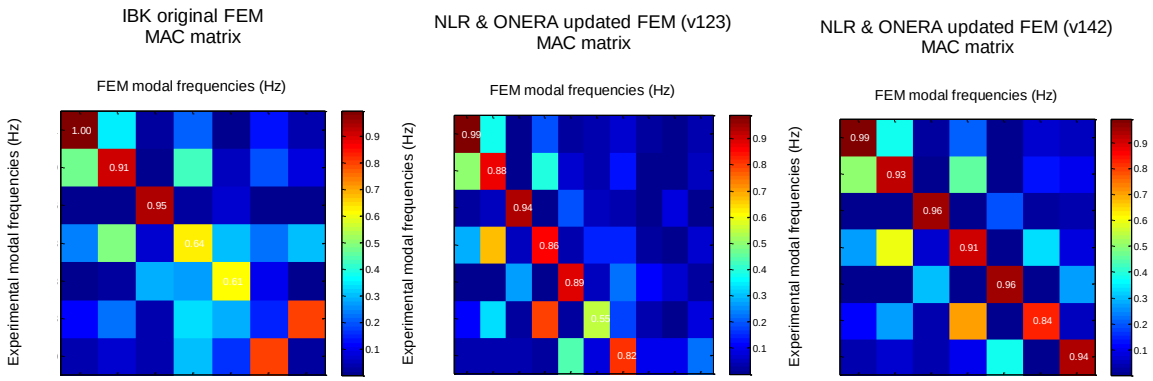

Figure 5 - Status after ONERA FEM fine-tuning – Rear blade – Dynamic results – MAC

		Δf/f	
Mode	IBK original	NLR updated	ONERA fine-tuned

1	-8.7 %	-8.4 %	0.9 %
2	-3.7 %	-12.3 %	2.7 %
3	-9.8 %	-13.7 %	-0.4 %
4	-11.1 %	-28.9 %	-3.3 %
5	-8.9 %	-11.6 %	-2.4 %
6	-	-25.1 %	-6.1 %

Table 1 - Status after ONERA FEM fine-tuning – Rear blade – Dynamic results - Frequencies

In our study, the structural problem is solved by the NASTRAN Sol400 solver on one processor. Two kinds of simulations were performed, direct linear or fully non linear approach, to measure the impact of structural nonlinearities on the hot shape computation.

2.3 Static coupling

The flowchart for the CFD/CSM static coupling is shown in figure 6. Once the flow has converged to a steady solution, the aerodynamic forces and moment are then extracted from the CFD grid to be interpolated on the CSM grid. This is done inside the aeroelastic interface. These structural loads are then injected as the source term in the CSM solver that will compute the displacements and velocities of the structure submitted to these loads. The aeroelastic interface will then interpolate these displacement and velocities from CSM grid to CFD grid aeroelastic interfaces and propagate the displacement in the aerodynamic volume mesh using a mesh deformation tool. This process is continued until convergence to equilibrium between the loads and the structural displacements.

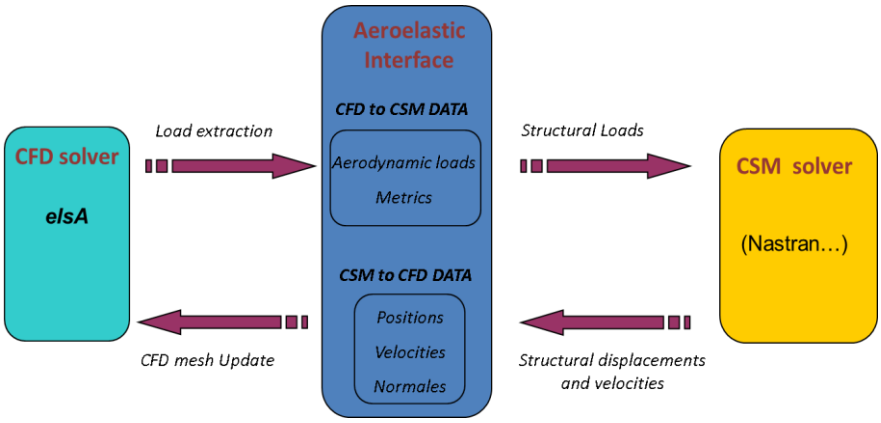

Figure 6: static coupling strategy

In term of wall clock time, the nonlinear approach for structure is more expensive than the linear one. More specifically, the wall clock time using linear approach is about 12.5 hours and close to16 hours using the nonlinear approach when solving the FEM problem.

3 RESULTS

During S1MA wind tunnel test campaign on Z49 CROR several quantities were extracted. The blade deflection, twist, and modal frequencies were deduced from SPA measurement as

presented in the first part of this study [1]. Static pressure coefficients, were also deduced from pressure transducer measurement. In this paper, these experimental key achievements are compared to the results of static aeroelastic computations.

3.1 Linear FEM Approximation

Nastran Sol400 linear computations are performed by setting the LGDISP parameter to -1. In these computations the centrifugal forces are also taken into account in a linear way.

Figure 7 compares SPA results (red curves) and aeroelastic computations using the linear approach (green curves) for the front blade. These results show that the linear approach overestimates by a factor of about 2 both the bending and twist at blade tip location meaning that the linear structural model is too flexible. If the shapes of the green and red curves are similar for the front blade, they differ concerning the rear blade twist.

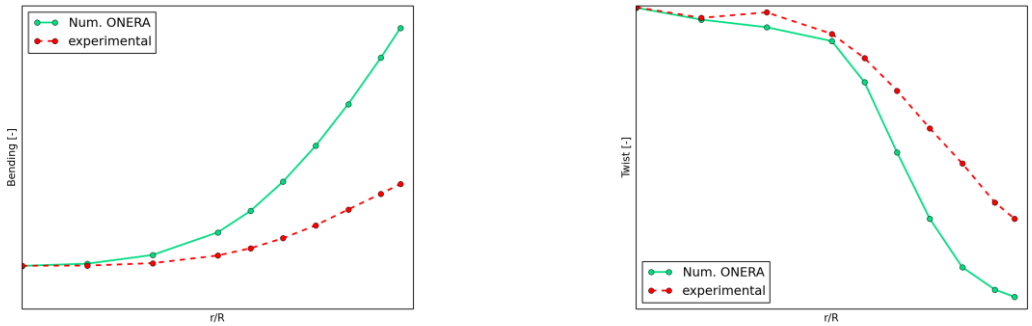

Figure 7 : Front blade : bending (left) and twist (right) as a function of normalized spanwise coordinate. Comparison between experimental, in red, and numerical, in green, results

Figure 8 reports on similar results but concerning the rear blade. The bending computed from numerical static coupling is also twice as big as the one found experimentally and are similarly shaped, the computed twist completely differ from experimental data. In the blade foot region the computed blade twist is close to zero but rapidly collapse after that point. On the contrary the curve resulting from experimental test results increases in the blade tip region and decreases in the other regions.

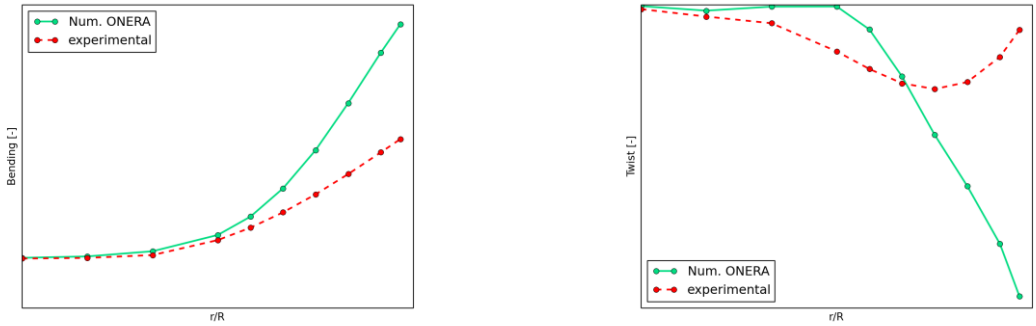

Figure 8 : Rear blade : bending (left) and twist (right) as a function of normalized chord coordinate. Comparison between experimental, in red, and numerical, in green, results

Oddly enough, these strong differences in displacement do not have a major impact on pressure distributions. A comparison of the experimental, red points, and numerical, blue curves, pressure distribution are shown figure 9 and figure 10 respectively for the front and rear blades. Concerning the front blade, the numerical simulation globally underestimates the static pressure coefficients on the pressure side and overestimates the pressure coefficients at the trailing edge of the suction side. For the rear blade, the numerical and experimental results are in fair agreement. Again in the middle part of the blade, the numerical simulation overestimates the pressure coefficients at trailing edge but with respect to the discrepancy between the numerical and experimental results in term of displacements, this fair agreement is surprising.

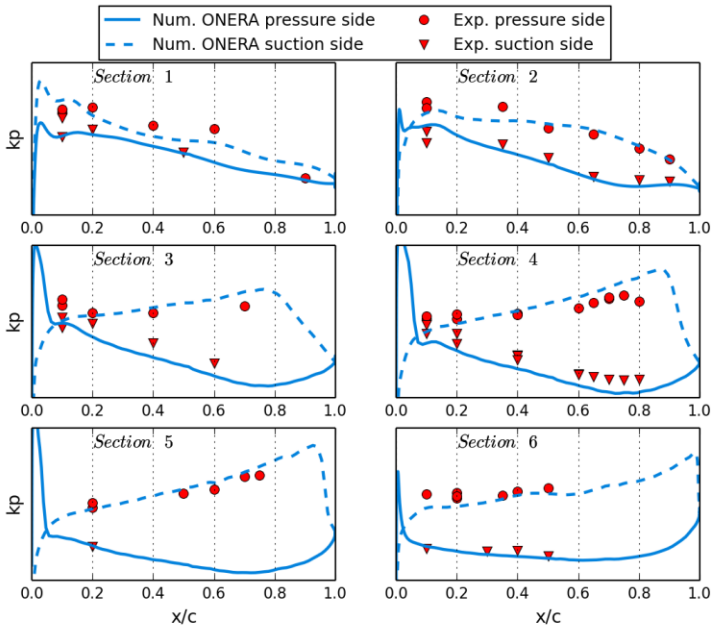

Figure 9: Front blade: Comparison between experimental and numerical pressure coefficient

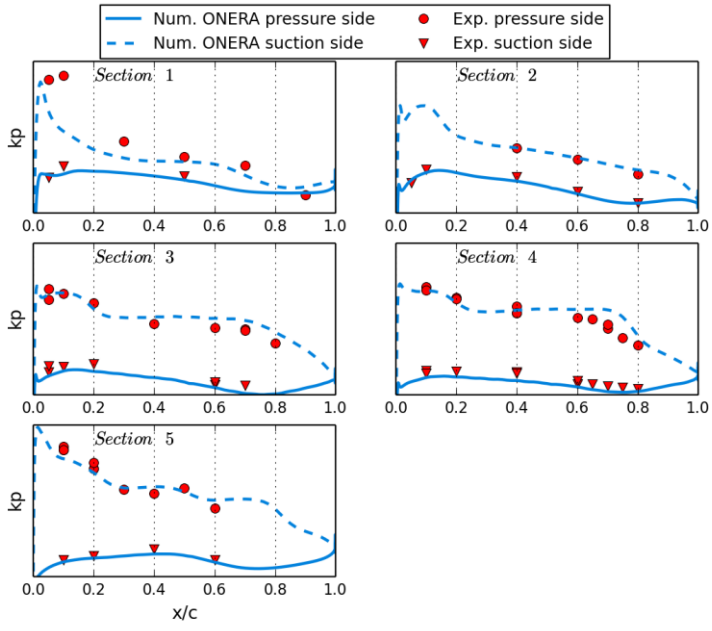

Figure 10: Rear blade: Comparison between experimental and numerical pressure coefficient

Finally, the modal frequencies of the hot shape have been computed and compared to those measured experimentally using strain gauges data. The relative error for the five first modes is shown on table 2. Again surprisingly, there is a relatively good agreement between experimental and numerical results. On both blades the maximum relative error is found for the torsion modes.

Mode	Description	Error, %, Front	Error,% Rear
1	First bending	-1.18	-3.6
2	Second bending	3.2	-0.8
3	First torsion	-4.7	-5.1
4	Third bending	2.2	-1.7
5	Second torsion	-6.8	2.9

Table 2: frequency error

The fair agreement between experimental and numerical result in term of pressure distribution and modal frequencies is misleading. Thanks to the experimental SPA data we can conclude that the linear approach is not sufficient to compute correctly the blade hot shape.

3.2 Nonlinear Approximation

In this part, static aeroelastic computations using a nonlinear approach for the structure part are performed. Two different FE models are considered. The first model is composed of the NLR Front blade FEM and ONERA rear blade FEM, and the second one is composed of the ONERA FEM for front and rear blade.

Figure 11 shows a comparison between SPA data (red curve), numerical results from NLR FEM (orange) and ONERA FEM (blue) for the front rotor blade. As far as bending is concerned, both ONERA and NLR model are very close and fairly agree with the experimental results. But both ONERA and NLR model fail to predict the twist in the hub region. However the numerical results fit better the experimental curve starting from the middle part of the blade span. In this region, the blue curve seems to fit better the experimental data than the orange curve but the shape of the latter curve seems to be more accurate. Both of these results show that the initial FEM model delivered by NLR is more flexible than the tuned one.

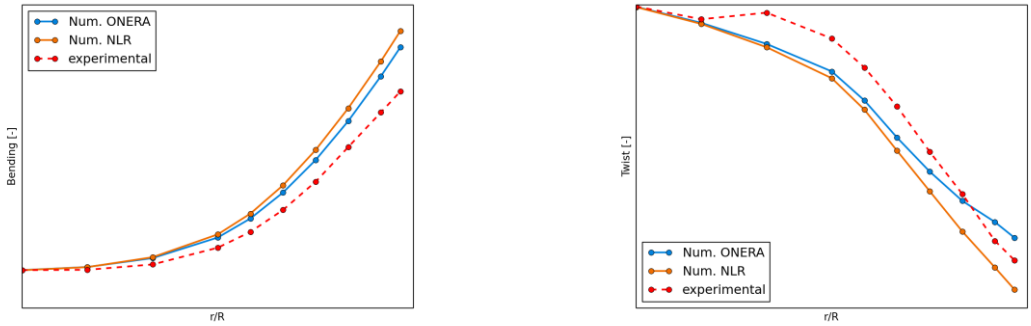

Figure 11: Front blade: bending (left) and twist (right) as a function of normalized chord coordinate.

Figure 12 shows the same comparison for the rear blade. As the FEMs are identical for the rear blade in both computations, the blade deflections are very similar. A fairly good agreement is found when comparing the numerical and experimental results for bending in term of shape or levels. Concerning the blade twist, as in the linear approach, the numerical and experimental results completely differ but the magnitudes are more accurate using the nonlinear approach. This particular result tends to show that the FEM model is not accurate for the rear blade.

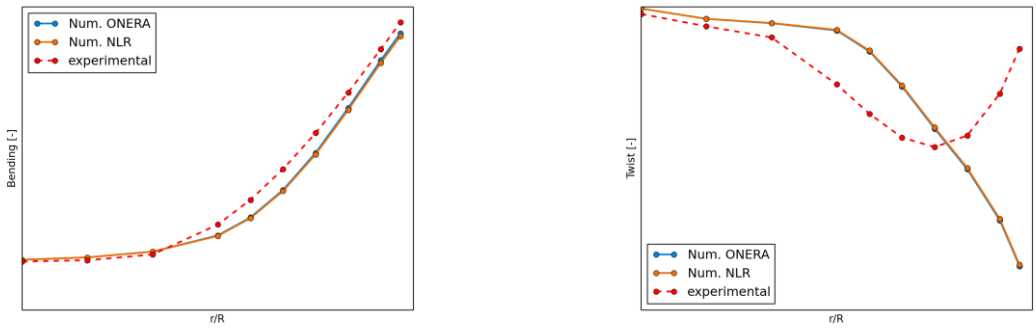

Figure 12 : Rear blade: bending (left) and twist (right) as a function of normalized chord coordinate.

The static pressure coefficient correlations are shown in figure 13 and figure 14 respectively for the front and rear blades. Compared to the results obtained from the linear approach these results lead to a better prediction of the pressure coefficient on the pressure side of the blade. Concerning the blade pressure side, as opposed to the previous results presented in figure 9 and figure 10, these results tend to underestimate the static pressure on this side of the blade.

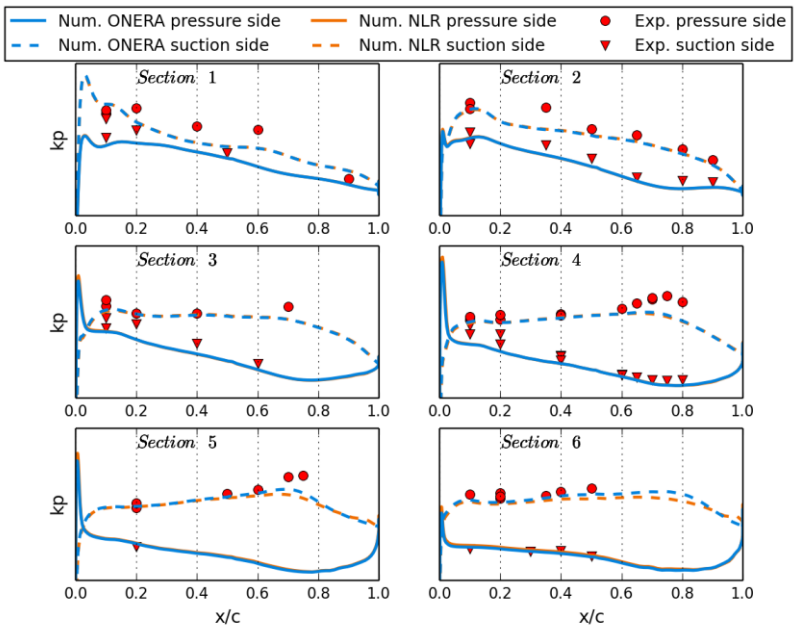

Figure 13: Front blade: Comparison between experimental and numerical static pressure coefficient

The impact of the greater flexibility of the NLR FEM front blade on the static pressure coefficient is only visible in the blade-tip region. In this region, on the blade pressure side, the ONERA model better fit the experimental results, especially in the rear part of the blade the ONERA model better predict the low pressure zone.

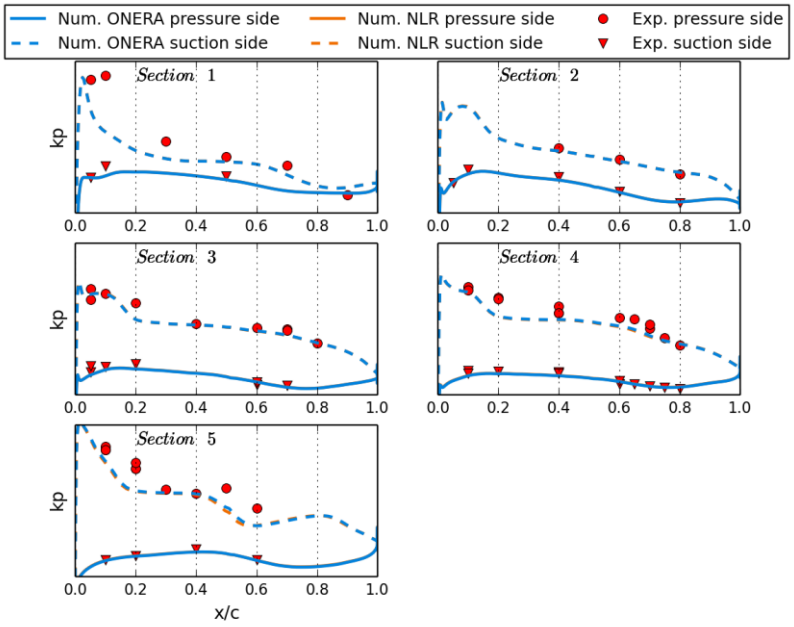

Figure 14: Rear blade: Comparison between experimental and numerical pressure coefficient

Concerning the poor correlation of the static pressure coefficient in the hub zone for the front and the rear blade, it can be explained by the use of a two equation turbulence model. Indeed, it is well known that this kind of model fails at predicting the flows in the region where curvature effect strongly influences the flow.

Finally, a modal analysis has been performed on the hot shape on both ONERA and NLR FEMs and the modal frequencies are compared, in term of relative error, to experimental

results. As the blade displacements of the two FEMs models are very similar the relative error on modal frequencies are also comparable. Compared to the frequencies obtained from aeroelastic computation using a linear approach and presented in table 2, the nonlinear approach only improves the frequencies of the torsion modes but slightly deteriorates the frequencies of bending modes.

Mode	Description	Error, %, Front blade		Error,% Rear blade	
		NLR	ONERA	NLR	ONERA
1	First bending	-3.8	-4.	2.3	2.4
2	Second bending	-3.6	-4.3	5.4	5.3
3	First torsion	-2.2	-3	0.5	0.4
4	Third bending	-2.2	-1.8	0.4	0.4
5	Second torsion	-1.	-1.	2.0	2.1

Table 3: frequency error

4 SUMMARY AND CONCLUSIONS

Three different aeroelastic computations were performed and compared to experimental data. The first static aeroelastic analysis was performed considering a linear approach for the FEM model. The results showed that if the frequencies and static pressure coefficients were comparable to the experimental results, the displacements were largely overestimated. These results tend to show that the linear hypothesis made on the structural behavior leads to serious error in blade displacement predictions.

The two other static aeroelastic computations were performed using non linear simulations for the structure part. The only difference between the two calculations was the FEM model. The first one was delivered to ONERA by NLR, the second is the same model statically and dynamically tuned using laboratory tests. Aeroelastic computations using these models were in relatively good agreement in term of displacements, static pressure and frequencies with experimental data. Results obtained with the tuned FEM model were slightly better.

5 ACKNOWLEDGEMENTS

This work has been undertaken within the Joint Technology Initiative “JTI CleanSky”, Smart Fixed Wing Aircraft Integrated Technology Demonstrator “SFWA-ITD” project (contract N°

CSJU-GAM-SFWA-2008-001) financed by the 7th Framework programme of the European Commission.

6 REFERENCES

[1] Geeraert A., Stephan C., *CROR Blade deformation, part 1: Experimental results by Strain Pattern Analysis*, IFASD-2015-023, June 2015

[2] Negulescu C., Airbus AI-PX7 CROR Design Features and Aerodynamics, SAE int. J. Aerosp. 6(2), 2013, DOI:10.4271/2013-01-2245

[3] Cambier L., Veuillot J. P., Status of the elsA cfd software for flow simulation and multidisciplinary applications, *46th AIAA Aerospace Science Meeting and exhibit*, number 664, 2008.

[4] Jameson A., Schmidt W., and Turkel E., Numerical solution of the Euler equations by finite volume methods using Runge-kutta time stepping schemes, *AIAA 14th Fluid and Plasma Dynamics Conference*, 1981.

[5] Kok J. C., resolving the dependence on freestream values for the k-ω turbulence model, *AIAA Journal, Vol. 38, No. 7, pp. 1292-1295*, August 2000.

[6] Yoon S. and Jameson A., An LU-SSOR scheme for the Euler and Navier-stokes equations, *In AIAA 25th Aerospace Sciences Meeting*, 1987.

[7] Stürmer A, Akkermans R.A.D., Multidisciplinary analysis of CROR propulsion systems: DLR activities in the JTI SFWA project, *CEAS Aeronautical Journal, vol 5, No. 3, pp 265-277, 2014*

[8] Dugeai A., Mauffrey Y., SICOT F., Aeroelastic capabilities of the elsA solver for rotating machines applications, *IFASD 2011, paper 079, Paris, June*

7 COPYRIGHT STATEMENT